Talanta 221 (2021) 121379

Contents lists available at ScienceDirect

Talanta

journal homepage: www.elsevier.com/locate/talanta

Ultrasensitive electrochemiluminescence biosensor for the detection of tumor exosomes based on peptide recognition and luminol-AuNPs@g-C_3N_4 nanoprobe signal amplification

Xuejiao Liu [a], Qiaoe Wang [b], Jun Chen [a], Xu Chen [a,*], Wensheng Yang [a,**]

[a] State Key Laboratory of Chemical Resource Engineering, Beijing University of Chemical Technology, Beijing, 100029, PR China
[b] Key Laboratory of Cosmetic, Beijing Technology and Business University, China National Light Industry, Beijing, 100048, PR China

ARTICLE INFO

Keywords:
Exosomes
Phosphatidylserine
Peptide
Signal amplification
Electrochemiluminescence
Biosensor

ABSTRACT

Highly sensitive determination of tumor exosomes is significant for early diagnosis of cancers and precision therapy. Herein, a sandwich peptide-based electrochemiluminescence (ECL) biosensor was developed for determination of phosphatidylserine (PS)-positive exosomes, a promising biomarker for early diagnosis of ovarian malignancy. A PS-specific binding peptide with high affinity was immobilized on Au nanoflowers (AuNFs) modified biosensing interface for recognition and capture of exosomes. Meanwhile, g-C_3N_4 nanosheet loaded with luminol capped AuNPs (Lum-AuNPs@g-C_3N_4) nanocomposite was used as the ECL signal nanoprobe. The g-C_3N_4 nanosheets with large surface area were not only utilized as the carrier to immobilize more peptides for recognition of exosomes but also used to catalyze co-reactant H_2O_2 decomposition to achieve the ECL signal amplification of luminol-H_2O_2 system. Under optimal conditions, the biosensor showed superior performances compared with most currently available methods, including wider linear range across 5 orders of magnitude and a lower detection limit (LOD) down to 39 particles μL^{-1}. Moreover, the biosensor could be applicable for determination of exosomes in complex biological samples. This study indicates the combination of peptide recognition with nanoprobe as a label for signal amplification in sandwich ECL biosensing is a great promising strategy for sensitive and cost-effective determination of exosomes.

1. Introduction

Exosomes are nanoscale extracellular vesicles (30–150 nm in diameters) containing various molecular constituents like lipids, nucleic acids and proteins from originating cells and play an important role in intercellular communication [1,2]. More importantly, exosomes are involved in tumorigenesis and cancer metastasis [3], and have become potential noninvasive biomarkers for cancer early diagnosis [4,5]. Ovarian malignancy is the deadliest female malignancy. Most patients are diagnosed at the advanced-stage owing to lack of applicable markers for early clinical diagnosis [6]. Recently, it has been proved levels of phosphatidylserine (PS)-positive exosomes in the blood samples can distinguish healthy group and benign ovarian disease patients from ovarian malignancy patients [7,8], which confirmed the clinical value of PS-positive exosome as a promising early diagnostic biomarker for ovarian malignancy [9,10]. Enzyme-linked immunosorbent assay (ELISA) has been employed to analyze PS-positive exosomes [9,11]. However, these established assays are confined by the requirements of relatively large-volume samples, extensive technical operations as well as limited sensitivity [12,13]. Moreover, PS molecular recognition elements (i.e., annexin V, β2GP1 and KL15C) used in these two studies have some certain defects such as Ca^{2+}-dependence, low affinity, unsatisfactory stability or complicated preparation process. In consequence, it is imperative to develop simple, economical, effective and sensitive methods with novel recognition elements for the determination of PS-positive exosomes.

Until now, many methods have been developed for determination and analysis of exosomes, such as flow cytometry [14], colorimetric [15], fluorescence [16], surface-enhanced Raman scattering (SERS) [17], microfluidic [18] and electrochemical [19,20]. In addition, ECL method, which combines the advantages of electrochemical and chemiluminescence techniques, like simple instrumentation, high sensitivity,

* Corresponding author.
** Corresponding author.
E-mail address: chenxu@mail.buct.edu.cn (X. Chen).

https://doi.org/10.1016/j.talanta.2020.121379
Received 29 February 2020; Received in revised form 1 July 2020; Accepted 4 July 2020
Available online 18 July 2020

extensive dynamic range and affordable cost [21], has drawn great interest in its application in exosomes determination in the past two years. For example, Zhang's group developed an ECL aptasensor for exosomes determination based on CD63 aptamer-immobilized Eu^{3+}-doped CdS nanocrystals as ECL emitters [22]. Wang's group developed an ECL aptasensor for exosomes determination based on CD63 aptamer immobilized Ti_3C_2 MXenes nanosheets used as a probe [23]. More recently, Liu's group reported an ECL biosensor for analyzing exosomes on the basis of multivalent platform of GPC1 antibody immobilized Poly(amidoamine) dendrimer coated Au nanoparticles for exosomes capture [24]. These studies demonstrate that ECL technique provides feasibility for the determination of exosomes. However, the exosomes recognition elements (antibody and aptamer) employed in these approaches have some drawbacks, such as difficulty in site specific bioconjugation or restricted target range [25], which may limit the widespread application of the ECL method in determination of exosomes.

In recent years, using affinity peptides as recognition elements in the development of new bioassay systems has drawn increasing attention [26]. Compared with other biorecognition entities (antibody, receptor protein and aptamer), peptides exhibit many attractive advantages, including cost-effectiveness, facile synthetic technique without complicated purification procedures, broad target range, high specificity and binding affinity with simple chemical structure, easy modification and functionalization as well as excellent stability and reliability even in harsh environments [27,28]. Based on these merits, great advances have been made in peptide-based biosensors [29]. For instance, Park's group designed a label-free peptide-based electrochemical sensor for human norovirus determination [30]. Chai's group constructed a sensitive sandwich peptide-based ECL sensor for Cyclin A_2 determination [31]. The inherent advantages of the recognition peptides make them have enormous potential in the development of biosensors with outstanding performance.

Here, a sandwich peptide-based ECL sensor with graphitic phase carbon nitride nanosheet loaded with luminol capped gold nanoparticles (Lum-AuNPs@g-C_3N_4) as the signal nanoprobe was developed for determination of PS-positive exosomes (Scheme 1). Specific binding peptide (FNFRLKAGAKIRFGRGC), which can selectively recognize PS with high affinity [32,33], was applied as a biological molecular recognition element. The PS-specific binding of the peptide is convenient without Ca^{2+}-dependent [32]. Au nanoflowers (AuNFs) were deposited on glassy carbon electrode (GCE) as effective sensing interface for peptide modification and further exosomes capture. The g-C_3N_4 nanosheet, a carbon-based two-dimensional (2D) nanomaterial with large specific surface areas [34], was not only serviced as the carrier to load more recognition peptides but also used to catalyze co-reactant H_2O_2 decomposition to realize the effective ECL signal amplification of classic luminol-H_2O_2 system. The ECL biosensor enabled highly sensitive PS-positive exosomes determination and allowed for accurate and quantitative analysis of ovarian tumor cell-derived exosomes in complicated biological sample, showing great potential for clinical application.

2. Experimental

2.1. Reagents and materials

A PS-specific peptide FNFRLKAGAKIRFGRGC (17 mer, MW = 1941.34, lyophilized powder, purity >95%) was bought from Top-Peptide Biotechnology Co. Ltd. (Shanghai, China). The underlined sequence can selectively recognize PS with high affinity [32,33]. The thiol-containing cysteine in terminal of this peptide provides a terminal which can bind to gold for immobilization of the peptide. Bovine serum albumin (BSA, lyophilized powder, 96%), Chloroauric acid tetrahydrate ($HAuCl_4{\cdot}4H_2O$, 99.9%), Luminol (98.5%), $NaBH_4$ and melamine were purchased from Aladdin Reagent. All aqueous solutions were prepared with doubly distilled water (DDW).

2.2. Apparatus

Fluorescence spectrum was recorded on spectrophotometer (RF-5301PC, Shimadzu, Japan). Transmission electron microscopy (TEM) was determined by Hitachi HT7700 TEM. Dynamic light scattering (DLS) measurement and zeta potentials were determined on Zetasizer Nano ZS analyzer (Malvern, UK). The UV–vis absorption spectrum was

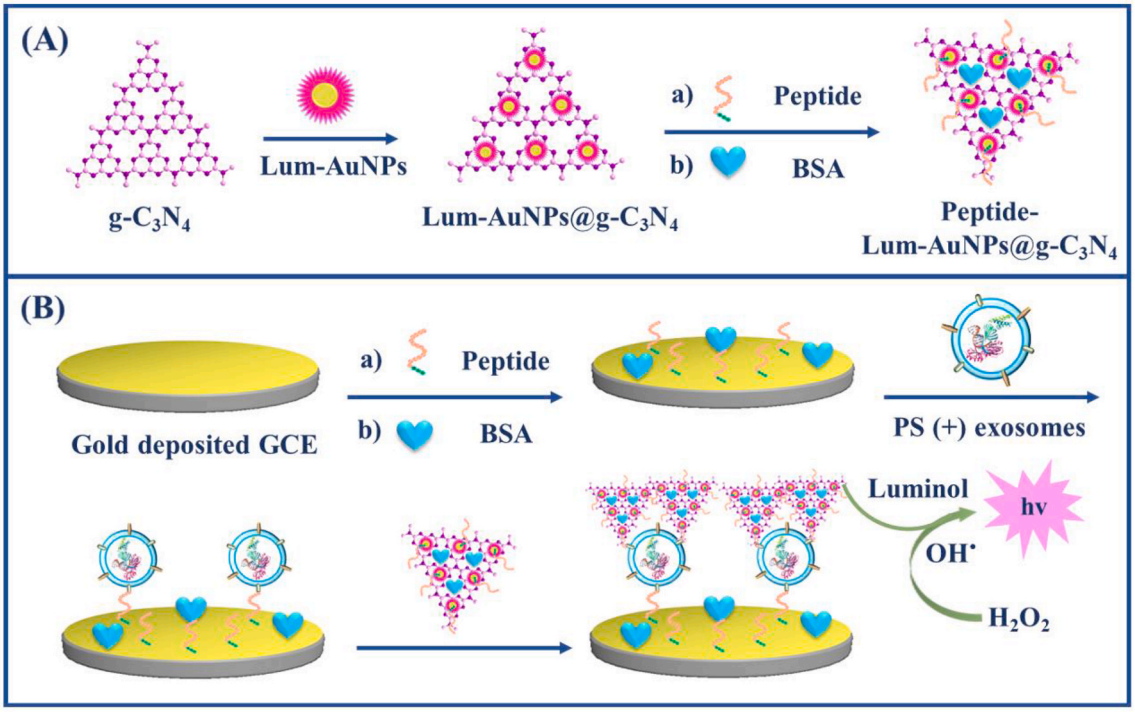

Scheme 1. (A) The preparation of peptide-Lum-AuNPs@g-C_3N_4 nanoprobe and (B) the construction of this ECL biosensor.

recorded by UV–vis spectrophotometer (PerkinElmer Lambda 35). Ultracentrifugation was performed on Beckman optima XPN-100 (Beckman, USA). Nanoparticle Tracking Analysis (NTA) were determined by NanoSight NS300 (Malvern Instruments). Electrochemical tests were recorded using CHI 660E electrochemical workstation (Shanghai, China). ECL tests were performed using MPI-Eelectrochemiluminescence analyzer (Xi'an Remex Analytical Instrument Ltd. Co., China). The voltage of photomultiplier tube (PMT) was set at 800 V. The range of scanning potential was 0.2–0.8 V at scan rate of 100 mV s^{-1}. Glassy carbon electrode (GCE, $\Phi = 3$ mm), Pt wire and Ag/AgCl were employed as working, auxiliary and reference electrode.

2.3. Synthesis of g-C_3N_4, Lum-AuNPs, Lum-AuNPs @g-C_3N_4 composites

The g-C_3N_4 nanosheet and Lum-AuNPs were synthesized according to the reported methods (S1.1-S1.2 in the experimental section of SI) [35,36]. And the Lum-AuNPs@g-C_3N_4 nanocomposite was synthesized via electrostatic interaction according to previous literature with some modifications [35]. Briefly, 5 mg positively charged g-C_3N_4 nanosheets were mixed with 5 mL as-prepared negatively charged Lum-AuNPs solution with gently stirred for 24 h. Then the obtained AuNPs/g-C_3N_4 were centrifuged at 6000 rpm, washed by DDW. Ultimately, the nanocomposite was dispersed in DDW and stored at 4 °C.

2.4. Synthesis of peptide-Lum-AuNPs@g-C_3N_4 nanoprobe

Peptide-Lum-AuNPs@g-C_3N_4 was prepared through mixing Lum-AuNPs@g-C_3N_4 and PS-specific peptide referring to the previous reports with some modifications [27,37]. As displayed in Scheme 1(A), 2 mL of Lum-AuNPs@g-C_3N_4 solution was mixed with 1 mL of 1 mM peptide followed stirring for 10 h at 4 °C to immobilize peptide on Lum-AuNPs@g-C_3N_4 by Au–S bond. Then 200 μL BSA solution (w/w, 1%) was added to the mixture for 1 h stirring to block non-specific binding site. Then the compound was centrifuged at 5000 rpm for 15 min by DDW and reconstructed in 1 mL DDW, and the peptide-Lum-AuNPs@g-C_3N_4 was obtained.

2.5. Cell culture and exosomes isolation

Ovarian tumor cell line SKOV3ip, non-cancerous human peritoneal mesothelial cell line HMrSV5 were growth in Roswell Park Memorial Institute (RPMI) 1640 containing 10% fetal bovine serum (FBS) at 37 °C in 5% CO_2. Exosomes were collected from cell culture supernatant by standard ultracentrifugation. Briefly, cells were harvested in exosome-free FBS-supplemented RPMI medium after 48 h. Next, the culture supernatant was centrifuged at 800×*g* for 5 min, 2000×*g* for 10 min to remove intact cell and cell debris. Afterwards, medium was filtered by 0.22 μm filters (Millipore Express PES Membrane, Carrigtwohill, Ireland). The filtered media was centrifuged at 100,000×*g* for 2 h at 4 °C. After the supernatant was removed, the exosome pellet was washed with phosphate buffered saline (PBS) and centrifuged at 100,000×*g* for another 2 h at 4 °C. Afterwards, sediment exosomes were resuspended in PBS. The purity as well as concentration of exosomes was measured by NanoSight. Stock solutions of 3.4 × 10^{12} particles mL^{-1} SKOV3ip-derived exosomes and 6.5 × 10^{10} particles mL^{-1} HMrSV5-derived exosomes were obtained, respectively.

2.6. Construction of the biosensor and detection of exosomes

The GCEs were polished with alumina slurries and sonicated in ethanol and DDW. Then, clean GCE was drenched into $HAuCl_4$ solution (w/v, 1%), and the AuNFs film modified electrode was obtained by electro-deposition at constant potential of −0.2 V for 30 s. Afterwards, the resulting gold deposited electrode was rinsed with DDW. Afterwards, the peptide was immobilized on the AuNFs/GCE surface by self-assembling technique. That was, the AuNFs/GCE was immersed in the assembly solution (1 μM PS-specific peptide) for 10 h at 4 °C, followed by washing. To block possible remaining active site, the pretreated electrode was dipped in BSA solution (w/w, 0.2%) for 30 min at 4 °C. Serial certain concentrations SKOV3ip exosomes solution with small volumes (6 μL) was incubated on the above electrode for 60 min. Unbound exosomes were removed by carefully rinsing with DDW. After that, 6 μL the peptide Lum-AuNPs@g-C_3N_4 nanoprobe was loaded on the exosomes captured electrode (exosomes/BSA/peptide/AuNFs/GCE), incubated for 60 min, and washed. At last, the modified electrode was measured by the ECL system in 0.1 M PBS (pH 7.4) (Na_2HPO_4–NaH_2PO_4–NaCl) containing 10 mM H_2O_2.

3. Results and discussion

3.1. Characterization of different nanomaterials

The g-C_3N_4 nanosheets was prepared and further characterized as displayed in Fig. 1. The TEM characterization in Fig. 1A shows the g-C_3N_4 nanosheets present the two-dimensional sheet-like structure. DLS data indicated that the average hydration size of g-C_3N_4 nanosheets was about 93 nm (Fig. S1). The fluorescence spectrum of synthesized g-C_3N_4 nanosheet under excitation 220–410 nm was also evaluated (Fig. 1B). Compared with bulk g-C_3N_4, emission peak of g-C_3N_4 nanosheet shifted from 465 to 433 nm. The blue-shift of the emission peak could be due to quantum confinement effect caused by nanosheets with only one or two layers [38]. Moreover, the g-C_3N_4 nanosheets solution can remain excellent dispersibility and homogeneity after being stored at 4 °C for several months (Fig. S2), making it favorable for biosensing applications.

After modification of Lum-AuNPs, as demonstrated in Fig. 1C, Lum-AuNPs were facilely deposited on g-C_3N_4 nanosheet. Lum-AuNPs@g-C_3N_4 nanocomposite was synthesized through electrostatic interactions with negatively charged Lum-AuNPs and positively charged g-C_3N_4 nanosheet (zeta potentials of g-C_3N_4 and Lum-AuNPs were exhibited in Fig. S3). Simultaneously, UV–vis spectrum was employed for confirming the load of Lum-AuNPs onto g-C_3N_4 nanosheet. As demonstrated in Fig. 1D, the Lum-AuNPs and Lum-AuNPs@g-C_3N_4 nanocomposite all showed three typical absorption peaks at 222 nm, 300 nm and 349 nm as well as one absorption band at 520 nm, which were corresponded to luminol and AuNPs, respectively [39], demonstrating Lum-AuNPs were successfully modified on surface of g-C_3N_4 nanosheet. Besides, the morphology of electrodeposited AuNFs was characterized by SEM. As depicted in Fig. S4, flower-like gold nanoparticles were uniformly distributed on the surface of GCE with an average diameter about 339.06 nm.

3.2. Characterization of exosomes

SKOV3ip cell-derived exosomes, which were PS positive [40], were employed as model exosomes in this work. The TEM (negative staining) observation was employed to characterize the morphology of isolated exosomes (S1.3 in the experimental section of SI). The diameters (Fig. S5) of purified exosomes were distributed in 40–80 nm, which were in agreement with reported size distribution range of exosomes [41]. NTA was also applied to confirm the hydrodynamic diameter distribution of collected exosomes (Fig. S6). The mode size of exosomes was around 119 nm, which was much bigger than that displayed in TEM because of optical scattering from solution [42].

3.3. Electrochemical characterization of this proposed biosensor

In order to characterize the construction procedure of the sensor, the cyclic voltammograms (CVs) of each modification steps were recorded. The CV curves were displayed in Fig. 2A. The well-behaved redox peaks of $Fe(CN_6)^{3-}/^{4-}$ redox couple were obtained from the bare GCE (curve a). Due to excellent conductivity of electrodeposited AuNFs modified on

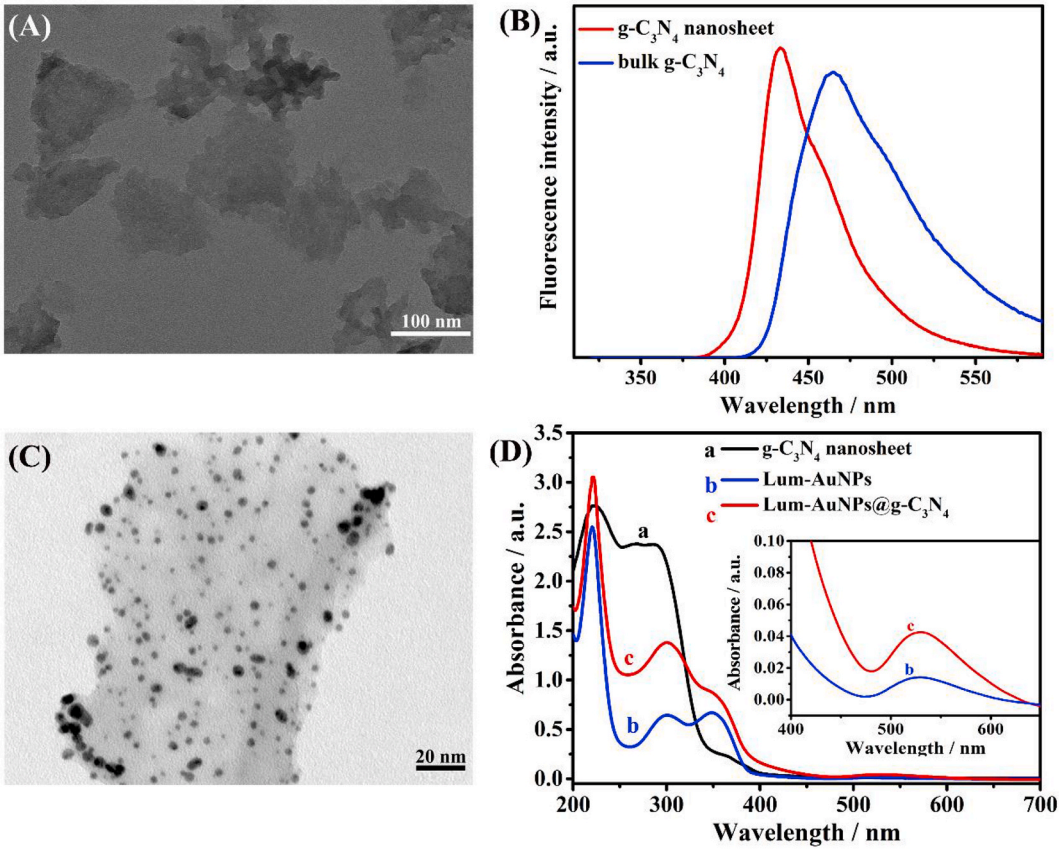

Fig. 1. (A) TEM characterization of g-C_3N_4 nanosheet. (B) Fluorescence emission spectrum of bulk g-C_3N_4 and g-C_3N_4 nanosheet. (C) TEM image of Lum-AuNPs@g-C_3N_4 nanocomposite. (D) UV–vis spectrum of g-C_3N_4 nanosheet (curve a), Lum-AuNPs (curve b) and Lum-AuNPs@ g-C_3N_4 (curve c).

GCE, obviously rising redox peak current was appeared (curve b). When PS-specific peptide was assembled onto AuNFs/GCE, the redox peak current declined due to steric hindrance effect of peptide (curve c). Then the electrode was incubated with BSA (curve d) and SKOV3ip exosomes (curve e), and the redox peak current successively declined, which was ascribed to the insulated effect of BSA and exosomes that hindered the electron transfer. When the synthesized nanocomposite peptide-Lum-AuNPs@g-C_3N_4 was incubated onto the modified GCE, current peak decreased further, showing that the signal nanoprobe had been successfully captured onto the electrode (curve f). Meanwhile, the electrochemical impedance spectroscopy (EIS) was also used for determining the stepwise assembly procedure of this biosensor and the Randles equivalence circuit was employed to simulate the EIS data. As displayed in Fig. 2B, electron transfer resistance (R_{ct}) value of the AuNFs/GCE (32.9 Ω, curve b) was smaller than bare GCE (90.7 Ω, curve a) due to favorably conductivity of AuNFs. After that, when the capture probe peptide, BSA, exosomes and the nanocomposite peptide-Lum-AuNPs@g-C_3N_4 were further modified on the AuNFs modified electrode, the R_{ct} values increased continuously and were 180.9 Ω, 294.5 Ω, 372.5 Ω and 512.0 Ω, respectively (Fig. 2B, curve c, d, e, f). These results were consistent with the outcomes in CVs, which indicate that the biosensor was successfully constructed.

3.4. Optimization of the conditions

To acquire better analytical performances of this proposed biosensor, the analytical conditions, including concentration of the co-reactant H_2O_2, the concentration of the capture peptide, the incubation time of exosomes and the incubation time of the peptide-Lum-AuNPs@g-C_3N_4 nanoprobe were optimized by a single variable method, and the optimized conditions were 10 mM,1 μM, 60 min and 60 min, respectively. To ensure the accuracy of the obtained optimized conditions, the analytical conditions of the biosensor were optimized again under these conditions. Firstly, concentration of H_2O_2 was investigated (Fig. S7A). Maximal ECL intensity was observed at H_2O_2 concentration of 10 mM, which was selected as optimal concentration of H_2O_2 for the determination of exosomes. Meanwhile, the concentration of capture peptide was also optimized. As indicated in Fig. S7B, the ECL intensity reached a maximum when the concentration of capture peptide was 1 μM, which was chosen as the optimal condition. Moreover, the incubation time of exosomes was an important effect factor. Fig. S7C displayed the ECL intensity showed a rising tendency with increasing incubation time of exosomes until 60 min. And the incubation time of the peptide-Lum-AuNPs@g-C_3N_4 nanoprobe was another important influence condition. As shown in Fig. S7D, the ECL intensity obviously rose with incubation time extension until it reached the maximum at 60 min. Thus, 60 min was selected for the following measurements. It can be seen from Fig. S7 that the maximum ECL values corresponding to each optimized condition were basically consistent, which indicated that the obtained conditions were indeed the optimal conditions.

3.5. ECL mechanisms of amplification strategies

To investigate the ECL signal amplification property of the proposed biosensor in PS-positive exosomes detection, biosensors with two different signal nanoprobes were fabricated under the same condition. As exhibited in Fig. 3, compared to the biosensor with peptide-Lum-AuNPs nanoprobe, ECL response (5940 a.u.) of the biosensor with peptide-Lum-AuNPs@g-C_3N_4 nanoprobe enhanced by about 2.4-fold. The ECL signal enhancement can be explained as follows: On the one hand, the g-C_3N_4 nanosheet with large surface area could provide more binding sites for immobilizing Lum-AuNPs and peptide. On the other

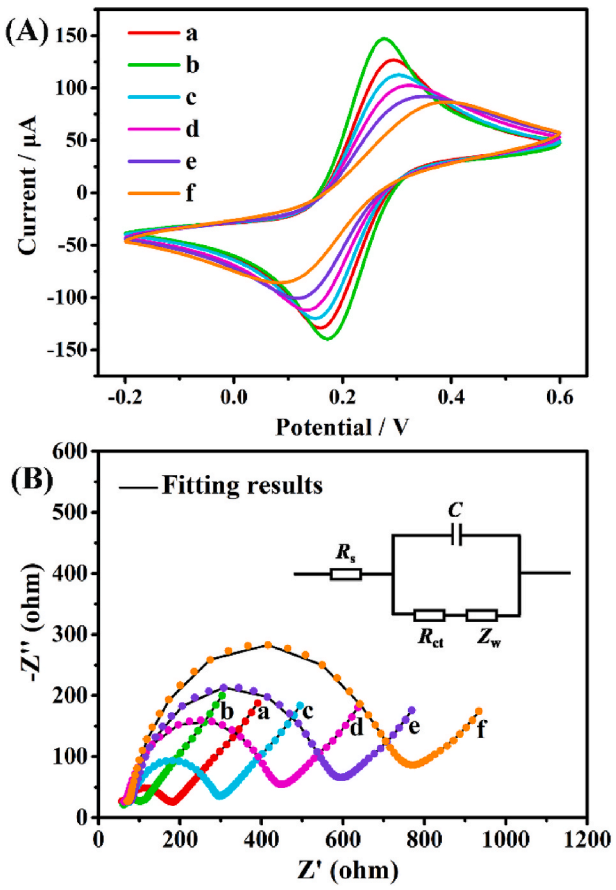

Fig. 2. (A) CVs and (B) EIS responses of various electrodes in 5 mM Fe $(CN_6)^{3-/4-}$ solution. (a) bare GCE, (b) AuNFs/GCE, (c) peptide/AuNFs/GCE, (d) BSA/peptide/AuNFs/GCE, (e) exosomes/BSA/peptide/AuNFs/GCE, (f) peptide-Lum-AuNPs@g-C_3N_4/exosomes/BSA/peptide/AuNFs/GCE. The scan rate of CV was 100 mV s^{-1}. The frequency range of EIS was 0.01 Hz–100 kHz. Inset of Fig. 2B displays an equivalent circuit: resistance offered by the electrolyte (R_s), double layer capacitance (C_d), electron transfer (R_{ct}) and Warburg component (Z_w).

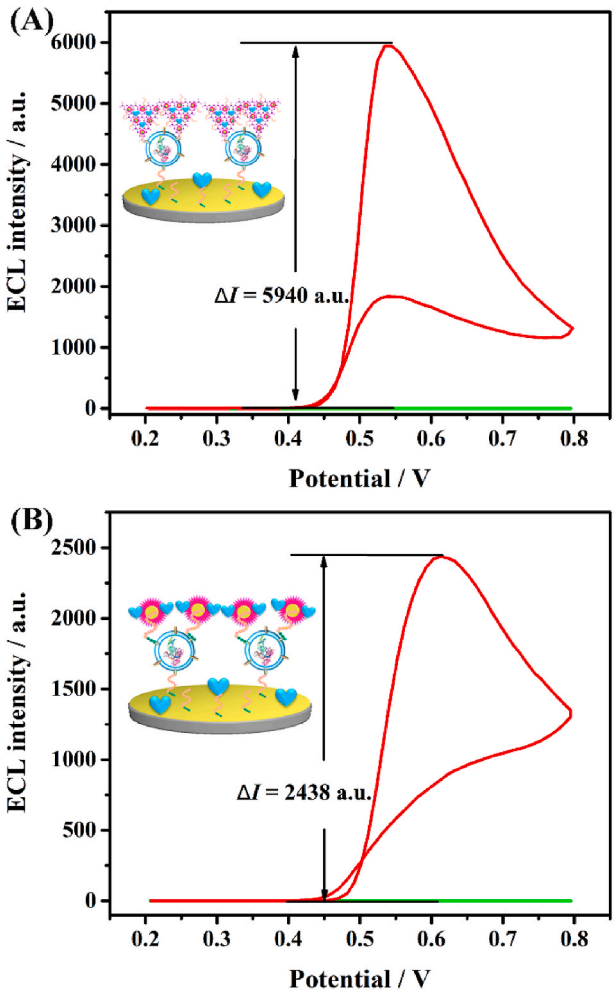

Fig. 3. ECL signal responses of biosensors toward exosomes of 1.0 × 10^6 particles μL^{-1} with different signal nanoprobes: (A) peptide-Lum-AuNPs@g-C_3N_4 nanoprobe and (B) peptide-Lum-AuNPs nanoprobe. The green and red line exhibited the ECL signals in absence and existence of nanoprobe, respectively. (For interpretation of the references to color in this figure legend, the reader is referred to the Web version of this article.)

hand, g-C_3N_4 nanosheet can show excellent catalytic activity in the decomposition of H_2O_2 to produce more reactive oxygen species like $OH^{\bullet}$ radicals [38,43], which could significantly boost the signal of luminol-H_2O_2 ECL system [44–46]. And according to previous works [47,48], the possible ECL mechanism is proposed. Initially, as displayed in Eq. (1), g-C_3N_4 as an effective catalyst facilitated the decomposition of H_2O_2 to produce $OH^{\bullet}$, which can react with luminol subsequently. As described in Eqs. (2) and (3), the generated $OH^{\bullet}$ as an oxidant could react with luminol$^{\bullet-}$ to form oxidized excited state (luminol$_{ox}$)*. Finally, the excited state (luminol$_{ox}$)* returned to the ground state luminol$_{ox}$ accompanied by an orange red 425 nm light (Eq. (4)).

$$H_2O_2 + e^- \rightarrow OH^{\bullet} + OH^- \quad (1)$$

$$\text{luminol} \rightarrow \text{luminol}^{\bullet-} \quad (2)$$

$$\text{luminol}^{\bullet-} + OH^{\bullet} \rightarrow (\text{luminol}_{ox})^* + \text{products} \quad (3)$$

$$(\text{luminol}_{ox})^* \rightarrow \text{luminol}_{ox} + h\nu \quad (4)$$

3.6. Analytical performance of this biosensor

Under optimal conditions, this sandwich ECL sensor was used for determination of SKOV3ip exosomes. Fig. 4A depicted the ECL Intensity−Time curves at different concentrations of SKOV3ip exosomes. The ECL intensity increased with the enhancing exosomes concentration. And calibration plot (Fig. 4B) displayed good linear relationship between signal intensity and the logarithm of SKOV3ip exosomes concentration from 1.0 × 10^2 to 1.0 × 10^7 particles μL^{-1} with limit of detection (LOD) down to 39 particles μL^{-1} (S/N = 3). Linear regression equation is $I = 1212.2 \lg c - 1439.49$ with the correlation coefficient of 0.9975. The LOD of the proposed ECL biosensor was much lower than that of the reported ELISA method for the detection of PS-positive exosomes [9,11,49]. Moreover, compared with other reported ECL and many other biosensors for detection of exosomes (Table S1), this peptide-based ECL biosensor showed wider linear range and lower detection limit. The excellent performances of this sensor could attribute to high specific recognition of the peptide to PS-positive exosomes and the signal amplification of peptide-Lum-AuNPs@g-C_3N_4 nanoprobe. More specifically, on the one hand, this biosensor utilized smaller size of peptide to instead of common PS recognition elements (i.e., annexin V, β2GP1 and KL15C), which reduced the distance between signal probe and electrode surface and improved the stability of system, resulting high detection sensitivity. On the other hand, Lum-AuNPs@g-C_3N_4 nanoprobe showed significant ECL signal amplification owing to high surface area and excellent H_2O_2 catalytic property of the g-C_3N_4 nanosheet. Based on above advantages, the biosensor demonstrated high sensitivity for SKOV3ip exosomes determination.

The ECL stability of the developed biosensor was studied in this

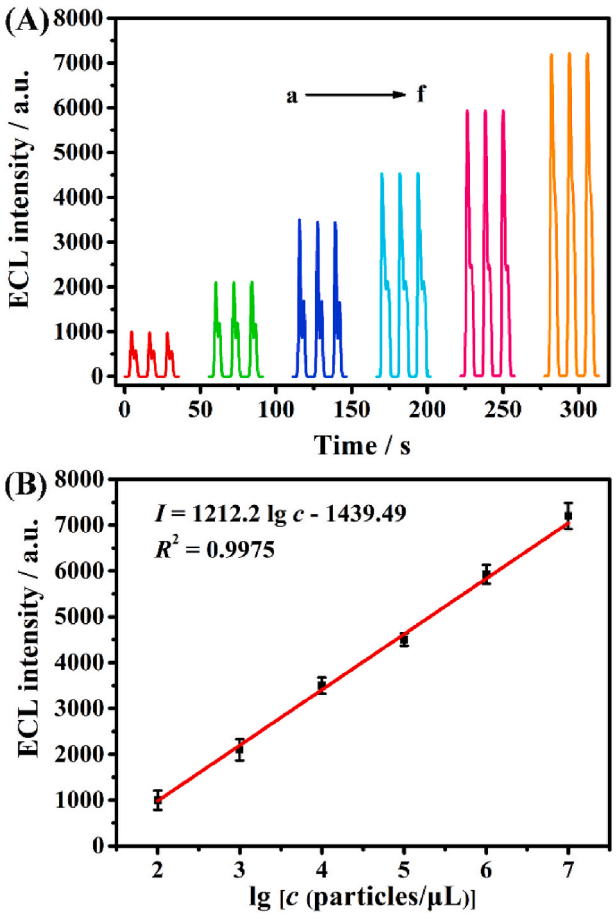

Fig. 4. (A) ECL signals of sensor for different concentrations of SKOV3ip cell-derived exosomes (a–f: 1.0×10^2, 1.0×10^3, 1.0×10^4, 1.0×10^5, 1.0×10^6, 1.0×10^7 particles μL^{-1}). (B) Calibration plot of the sensor for SKOV3ip cell-derived exosomes detection.

work. Fig. S8 displayed the ECL signal of the sensor was stable during successive scans, showing this sensor had good stability. Meanwhile, the reproducibility of different electrodes from the same batch was investigated. The relative standard deviation (RSD) of this sensor for 1.0×10^6 particles μL^{-1} of SKOV3ip exosomes was 4.6% (n = 3), which indicating the designed biosensor exhibited good reproducibility.

3.7. Determination of exosomes in biological sample

To assure the potential of this biosensor in clinical application, SKOV3ip exosomes were detected in exosome-free FBS, was used to examine the performance of this biosensor. As displayed in Fig. 5A, the result obtained from exosomes in PBS had no significant difference with that in exosome-free FBS (5%). Experimental result revealed the proposed biosensor could work in complex biological samples with good accuracy, indicating the potential application in clinical samples.

To verify the applicability of this biosensor for the determination of PS-positive exosomes, the proposed sensor was incubated with the same concentration of ovarian cancer cell SKOV3ip exosomes and non-cancerous human peritoneal mesothelial cell HMrSV5 exosomes. As shown in Fig. 5B, the ECL signal detected for SKOV3ip exosomes was about 6.7-fold larger than that for HMrSV5 exosomes determination. Calculated by the linear regression equation obtained in this work, PS level expressed on SKOV3ip exosomes (ca. 1.0×10^6 particles μL^{-1}) was about 6 orders of magnitude higher than that on HMrSV5 exosomes (ca. 66 particles μL^{-1}). The result proved that the level of PS-positive exosomes derived from cancer cell was much higher than that derived from non-cancerous cell, which was similar to that reported in the previous study [9], and showed that the developed biosensor had potential application value in the detection of PS-positive exosomes.

4. Conclusions

In summary, a novel ultrasensitive sandwich ECL biosensor was fabricated for determination of PS-positive exosomes. This ECL biosensor combines the advantages of peptide recognition and signal amplification of Lum-AuNPs@g-C_3N_4 nanoprobe. They were synergistically and significantly beneficial for highly efficient determine PS-positive exosomes to achieve a wide linear range across 5 orders of magnitude and low LOD down to 39 particles μL^{-1}. In addition, the biosensor can differentiate tumor exosomes from non-tumor exosomes. To the best of our knowledge, this is the first ECL sensor for PS-positive exosomes determination based on peptide recognition. This study will provide a new avenue to develop peptide-based biosensors for the analysis of exosomes.

Credit author statement

Xuejiao Liu: Conceptualization, Methodology, Writing-Original Draft. Qiaoe Wang: Supervision. Jun Chen: Investigation, Validation. Xu Chen: Data curation, Writing-Review & Editing, Resources. Wensheng Yang: Project administration, Visualization.

Declaration of competing interest

The authors declare that they have no known competing financial interests or personal relationships that could have appeared to influence the work reported in this paper.

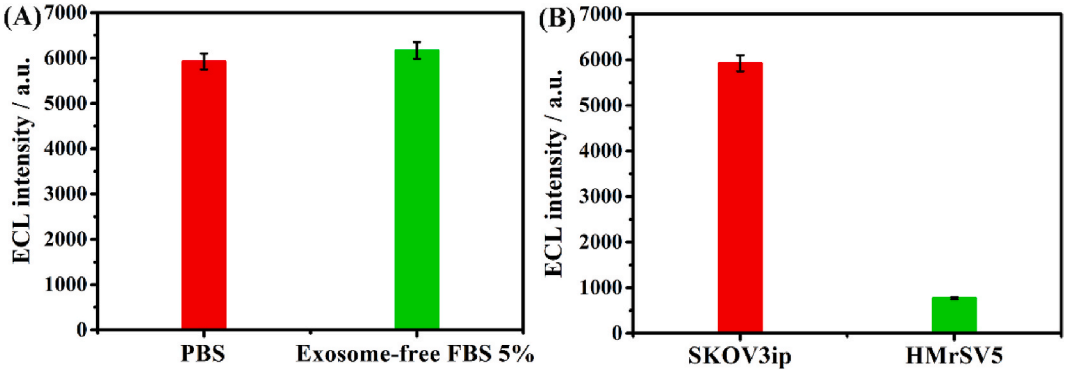

Fig. 5. (A) Detection of 1×10^6 particles μL^{-1} SKOV3ip cell-derived exosomes in PBS and 5% exosome-free FBS. (B) ECL responses of this sensor for exosomes secreted from SKOV3ip cell and HMrSV5 cell at the concentrations of 1×10^6 particles μL^{-1}.

Acknowledgments

This work was supported by National Natural Science Foundation of China (201874005 and 21521005), Open Research Fund Program of Key Laboratory of Cosmetic (Beijing Technology and Business University), China National Light Industry (No. KLC-2019-ZD3), Fundamental Research Funds for the Central Universities (XK1901) and Research projects on biomedical transformation of China-Japan Friendship Hospital (No. PYBZ1833).

Appendix A. Supplementary data

Supplementary data to this article can be found online at https://doi.org/10.1016/j.talanta.2020.121379.

References

[1] B.S. Chia, Y.P. Low, Q. Wang, P. Li, Z. Gao, Advances in exosome quantification techniques, TrAC Trends Anal. Chem. 86 (2017) 93–106.
[2] C.M. Boulanger, X. Loyer, P.-E. Rautou, N. Amabile, Extracellular vesicles in coronary artery disease, Nat. Rev. Cardiol. 14 (5) (2017) 259–272.
[3] K. Liang, F. Liu, J. Fan, D. Sun, C. Liu, C.J. Lyon, D.W. Bernard, Y. Li, K. Yokoi, M. H. Katz, E.J. Koay, Z. Zhao, Y. Hu, Nanoplasmonic quantification of tumour-derived extracellular vesicles in plasma microsamples for diagnosis and treatment monitoring, Nat. Biomed. Eng. 1 (4) (2017), 0021.
[4] S.H. Jalalian, M. Ramezani, S.A. Jalalian, K. Abnous, S.M. Taghdisi, Exosomes, new biomarkers in early cancer detection, Anal. Biochem. 571 (2019) 1–13.
[5] C. Liu, J. Zhao, F. Tian, L. Cai, W. Zhang, Q. Feng, J. Chang, F. Wan, Y. Yang, B. Dai, Y. Cong, B. Ding, J. Sun, W. Tan, Low-cost thermophoretic profiling of extracellular-vesicle surface proteins for the early detection and classification of cancers, Nat. Biomed. Eng. 3 (3) (2019) 183–193.
[6] L. Giannopoulou, M. Zavridou, S. Kasimir-Bauer, E.S. Lianidou, Liquid biopsy in ovarian cancer: the potential of circulating miRNAs and exosomes, Transl. Res. 205 (2019) 77–91.
[7] E. Carollo, B. Paris, P. Samuel, P. Pantazi, T.F. Bartelli, E. Dias-Neto, S.A. Brooks, R. C. Pink, D.R.F. Carter, Detecting ovarian cancer using extracellular vesicles: progress and possibilities, Biochem. Soc. Trans. 47 (1) (2019) 295–304.
[8] C. Yang, H.S. Kim, G. Song, W. Lim, The potential role of exosomes derived from ovarian cancer cells for diagnostic and therapeutic approaches, J. Cell. Physiol. 234 (12) (2019) 21493–21503.
[9] J. Lea, R. Sharma, F. Yang, H. Zhu, E.S. Ward, A.J. Schroit, Detection of phosphatidylserine-positive exosomes as a diagnostic marker for ovarian malignancies: a proof of concept study, Oncotarget 8 (9) (2017) 14395–14407.
[10] S. Sharma, F. Zuñiga, G.E. Rice, L.C. Perrin, J.D. Hooper, C. Salomon, Tumor-derived exosomes in ovarian cancer - liquid biopsies for early detection and real-time monitoring of cancer progression, Oncotarget 8 (61) (2017) 104687–104703.
[11] R. Sharma, X. Huang, R.A. Brekken, A.J. Schroit, Detection of phosphatidylserine-positive exosomes for the diagnosis of early-stage malignancies, Br. J. Canc. 117 (2017) 545.
[12] H. Im, H. Shao, Y.I. Park, V.M. Peterson, C.M. Castro, R. Weissleder, H. Lee, Label-free detection and molecular profiling of exosomes with a nano-plasmonic sensor, Nat. Biotechnol. 32 (5) (2014) 490–495.
[13] C. Liu, J. Zhao, F. Tian, J. Chang, W. Zhang, J. Sun, λ-DNA- and aptamer-mediated sorting and analysis of extracellular vesicles, J. Am. Chem. Soc. 141 (9) (2019) 3817–3821.
[14] Y. Tian, L. Ma, M. Gong, G. Su, S. Zhu, W. Zhang, S. Wang, Z. Li, C. Chen, L. Li, L. Wu, X. Yan, Protein profiling and sizing of extracellular vesicles from colorectal cancer patients via flow cytometry, ACS Nano 12 (1) (2018) 671–680.
[15] Y. Xia, M. Liu, L. Wang, A. Yan, W. He, M. Chen, J. Lan, J. Xu, L. Guan, J. Chen, A visible and colorimetric aptasensor based on DNA-capped single-walled carbon nanotubes for detection of exosomes, Biosens. Bioelectron. 92 (2017) 8–15.
[16] Y. Wang, D. Luo, Y. Fang, W. Wu, Y. Wang, Y. Xia, F. Wu, C. Li, J. Lan, J. Chen, An aptasensor based on upconversion nanoparticles as LRET donors for the detection of exosomes, Sensor. Actuator. B Chem. 298 (2019) 126900.
[17] M. Avella-Oliver, R. Puchades, S. Wachsmann-Hogiu, A. Maquieira, Label-free SERS analysis of proteins and exosomes with large-scale substrates from recordable compact disks, Sensor. Actuator. B Chem. 252 (2017) 657–662.
[18] P. Zhang, X. Zhou, M. He, Y. Shang, A.L. Tetlow, A.K. Godwin, Y. Zeng, Ultrasensitive detection of circulating exosomes with a 3D-nanopatterned microfluidic chip, Nat. Biomed. Eng. 3 (6) (2019) 438–451.
[19] Y.G. Zhou, R.M. Mohamadi, M. Poudineh, L. Kermanshah, S. Ahmed, T.S. Safaei, J. Stojcic, R.K. Nam, E.H. Sargent, S.O. Kelley, Interrogating circulating microsomes and exosomes using metal nanoparticles, Small 12 (6) (2016) 727–732.
[20] S. Wang, L. Zhang, S. Wan, S. Cansiz, C. Cui, Y. Liu, R. Cai, C. Hong, I.-T. Teng, M. Shi, Aptasensor with expanded nucleotide using DNA nanotetrahedra for electrochemical detection of cancerous exosomes, ACS Nano 11 (4) (2017) 3943–3949.
[21] X. Zhu, Q. Zhai, W. Gu, J. Li, E. Wang, High-sensitivity electrochemiluminescence probe with molybdenum carbides as nanocarriers for α-fetoprotein sensing, Anal. Chem. 89 (22) (2017) 12108–12114.
[22] B. Qiao, Q. Guo, J. Jiang, Y. Qi, H. Zhang, B. He, C. Cai, J. Shen, An electrochemiluminescent aptasensor for amplified detection of exosomes from breast tumor cells (MCF-7 cells) based on G-quadruplex/hemin DNAzymes, Analyst 144 (11) (2019) 3668–3675.
[23] H. Zhang, Z. Wang, Q. Zhang, F. Wang, Y. Liu, Ti_3C_2 MXenes nanosheets catalyzed highly efficient electrogenerated chemiluminescence biosensor for the detection of exosomes, Biosens. Bioelectron. 124–125 (2019) 184–190.
[24] Y. Zhang, F. Wang, H. Zhang, H. Wang, Y. Liu, Multivalency interface and g-C_3N_4 coated liquid metal nanoprobe signal amplification for sensitive electrogenerated chemiluminescence detection of exosomes and their surface proteins, Anal. Chem. 91 (18) (2019) 12100–12107.
[25] H. Li, H. Xie, Y. Cao, X. Ding, Y. Yin, G. Li, A general way to assay protein by coupling peptide with signal reporter via supermolecule formation, Anal. Chem. 85 (2) (2013) 1047–1052.
[26] J. Zhao, H. Chen, Y. Tang, H. Chen, G. Chen, Y. Yin, G. Li, Research progresses on the functional polypeptides in the detection and imaging of breast cancer, J. Mater. Chem. B 6 (17) (2018) 2510–2523.
[27] H. Qi, X. Qiu, D. Xie, C. Ling, Q. Gao, C. Zhang, Ultrasensitive electrogenerated chemiluminescence peptide-based method for the determination of cardiac troponin I incorporating amplification of signal reagent-encapsulated liposomes, Anal. Chem. 85 (8) (2013) 3886–3894.
[28] L. Yang, N. Li, K. Wang, X. Hai, J. Liu, F. Dang, A novel peptide/Fe_3O_4@ SiO_2-Au nanocomposite-based fluorescence biosensor for the highly selective and sensitive detection of prostate-specific antigen, Talanta 179 (2018) 531–537.
[29] A. Karimzadeh, M. Hasanzadeh, N. Shadjou, M.d.l. Guardia, Peptide based biosensors, TrAC Trends Anal. Chem. 107 (2018) 1–20.
[30] H.J. Hwang, M.Y. Ryu, C.Y. Park, J. Ahn, H.G. Park, C. Choi, S.-D. Ha, T.J. Park, J. P. Park, High sensitive and selective electrochemical biosensor: label-free detection of human norovirus using affinity peptide as molecular binder, Biosens. Bioelectron. 87 (2017) 164–170.
[31] H. Wang, Y. Yuan, Y. Chai, R. Yuan, Sandwiched electrochemiluminescent peptide biosensor for the detection of prognostic indicator in early-stage cancer based on hollow, magnetic, and self-enhanced nanosheets, Small 11 (30) (2015) 3703–3709.
[32] C. Xiong, K. Brewer, S. Song, R. Zhang, W. Lu, X. Wen, C. Li, Peptide-based imaging agents targeting phosphatidylserine for the detection of apoptosis, J. Med. Chem. 54 (6) (2011) 1825–1835.
[33] P. Miao, J. Yin, L. Ning, X. Li, Peptide-based electrochemical approach for apoptosis evaluation, Biosens. Bioelectron. 62 (2014) 97–101.
[34] S.G. Liu, L. Han, N. Li, Y.Z. Fan, Y.Z. Yang, N.B. Li, H.Q. Luo, A ratiometric fluorescent strategy for alkaline phosphatase activity assay based on g-C_3N_4/CoOOH nanohybrid via target-triggered competitive redox reaction, Sensor. Actuator. B Chem. 283 (2019) 515–523.
[35] Z. Guo, L. Wu, Y. Hu, S. Wang, X. Li, Potential-resolved "in-electrode" type electrochemiluminescence immunoassay based on functionalized g-C_3N_4 nanosheet and Ru-NH_2 for simultaneous determination of dual targets, Biosens. Bioelectron. 95 (2017) 27–33.
[36] J.-X. Wang, Y. Zhuo, Y. Zhou, R. Yuan, Y.-Q. Chai, Electrochemiluminescence immunosensor based on multifunctional luminol-capped AuNPs@Fe_3O_4 nanocomposite for the detection of mucin-1, Biosens. Bioelectron 71 (2015) 407–413.
[37] W. Li, L. Wu, X. Song, Y. Hu, S. Wang, X. Li, Z. Guo, Ultrasensitive and visual detection of squamous cell carcinoma antigen based on a silver-enhanced sandwich immunoassay using AuNPs@g-C_3N_4 nanocomposites, Sensor. Actuator. B Chem. 235 (2016) 670–677.
[38] Y.-M. Wang, J.-W. Liu, G.B. Adkins, W. Shen, M.P. Trinh, L.-Y. Duan, J.-H. Jiang, W. Zhong, Enhancement of the intrinsic peroxidase-like activity of graphitic carbon nitride nanosheets by ssDNAs and its application for detection of exosomes, Anal. Chem. 89 (22) (2017) 12327–12333.
[39] A. Zhang, W. Guo, H. Ke, X. Zhang, H. Zhang, C. Huang, D. Yang, N. Jia, D. Cui, Sandwich-format ECL immunosensor based on Au star@BSA-Luminol nanocomposites for determination of human chorionic gonadotropin, Biosens. Bioelectron. 101 (2018) 219–226.
[40] S. Keller, A.-K. König, F. Marmé, S. Runz, S. Wolterink, D. Koensgen, A. Mustea, J. Sehouli, P. Altevogt, Systemic presence and tumor-growth promoting effect of ovarian carcinoma released exosomes, Canc. Lett. 278 (1) (2009) 73–81.
[41] H. Dong, H. Chen, J. Jiang, H. Zhang, C. Cai, Q. Shen, Highly sensitive electrochemical detection of tumor exosomes based on aptamer recognition-induced multi-DNA release and cyclic enzymatic amplification, Anal. Chem. 90 (7) (2018) 4507–4513.
[42] H. Wang, H. Chen, Z. Huang, T. Li, A. Deng, J. Kong, DNase I enzyme-aided fluorescence signal amplification based on graphene oxide-DNA aptamer interactions for colorectal cancer exosome detection, Talanta 184 (2018) 219–226.
[43] Z. Wang, K. Dong, Z. Liu, Y. Zhang, Z. Chen, H. Sun, J. Ren, X. Qu, Activation of biologically relevant levels of reactive oxygen species by Au/g-C_3N_4 hybrid nanozyme for bacteria killing and wound disinfection, Biomaterials 113 (2017) 145–157.
[44] Y. Liu, H. Wang, C. Xiong, Y. Chai, R. Yuan, An ultrasensitive electrochemiluminescence immunosensor for NT-proBNP based on self-catalyzed luminescence emitter coupled with PdCu@carbon nanohorn hybrid, Biosens. Bioelectron. 87 (2017) 779–785.
[45] H. Sha, Y. Wang, Y. Zhang, H. Ke, X. Xiong, N. Jia, Enzyme-free ECL immunesensor based on PbS nanocrystals for highly sensitive detection of alpha fetoprotein, Sensor. Actuator. B Chem. 277 (2018) 157–163.
[46] J. Xu, D. Jiang, Y. Qin, J. Xia, D. Jiang, H.-Y. Chen, C_3N_4 nanosheet modified microwell array with enhanced electrochemiluminescence for total analysis of cholesterol at single cells, Anal. Chem. 89 (4) (2017) 2216–2220.

[47] H. Ke, X. Zhang, C. Huang, N. Jia, Electrochemiluminescence evaluation for carbohydrate antigen 15-3 based on the dual-amplification of ferrocene derivative and Pt/BSA core/shell nanospheres, Biosens. Bioelectron. 103 (2018) 62–68.
[48] L. Yang, J. Xue, Y. Jia, Y. Zhang, D. Wu, H. Ma, Q. Wei, H. Ju, Construction of well-ordered electrochemiluminescence sensing interface using peptide-based specific antibody immobilizer and N-(aminobutyl)-N-(ethylisoluminol) functionalized ferritin as signal indicator for procalcitonin analysis, Biosens. Bioelectron. 142 (2019) 111562.
[49] J. Webber, A. Clayton, How pure are your vesicles? J. Extracell. Vesicles 2 (1) (2013) 19861.